An Analytical Solution to the Problem of the Orientation of Rigid Particles by Planar Obstacles. Application to Membrane Systems and to the Calculation of Dipolar Couplings in Protein NMR Spectroscopy

Miguel X. Fernandes,[†,‡] Pau Bernadó,[‡,§] Miquel Pons,*[,§] and José García de la Torre*[,†]

Contribution from the Departamento de Química-Física, Universidad de Murcia, Campus de Espinardo, 30071 Murcia, Spain, and Departament de Química Orgànica, Universitat de Barcelona, Martí i Franquès, 1-11, 08028 Barcelona, Spain

Received June 4, 2001. Revised Manuscript Received September 28, 2001

Abstract: Nonspherical particles or molecules experience an ordering effect in the presence of obstacles due to the restrictions they place on the orientation of those molecules that are in their proximity. Obstacles may be the limits of a membrane in which the molecule is embedded, oriented mesoscopic systems such as bicelles, or membrane fragments used to induce weak protein alignment in a magnetic field. The overall shape of most proteins can be described to a good approximation by an ellipsoidal particle. Here we describe and solve analytically the problem of the orientation of ellipsoidal particles by planar obstacles. Simple expressions are derived for the orientational distribution function and the order parameter. These expressions allow the analytical calculation of the residual dipolar couplings for a protein of known three-dimensional structure oriented by steric effects. The results are in good agreement with experiment and with the results of previously described simulations. However, they are obtained analytically in a fraction of the time and therefore open the possibility to include the optimization of the overall shape in the determination of three-dimensional structures using residual dipolar coupling constraints. The equations derived are general and can also be applied to problems of a completely different nature. In particular, previous equations describing the orientation of particles embedded in membranes are verified and generalized here.

Introduction

The use of dipolar coupling as structural constraints has had an enormous impact on the determination of the structure of proteins by NMR.[1−3] The introduction of dipolar couplings increases the precision and the accuracy of the structures[4−6] and, when complemented with other long-range constraints such as those derived from paramagnetic effects or chemical shift information, may provide the fold of the protein even without NOE information.[7−9] The ease of assignment of dipolar couplings makes them obvious tools for NMR-based high-throughput strategies of protein structure determination.[10,11] The long-range angular information provided is crucial for the determination of the relative orientation of individual domains in multidomain protein or of individual proteins in multi-protein complexes.[12,13] However, long-range distance information, completing the characterization of the protein global shape, is only available indirectly from dipolar coupling measurements through the alignment tensor. Alternatively, relaxation time measurements may allow the characterization of the global shape through the rotational diffusion tensor. However, proper separation between global tumbling and internal motion can be nontrivial,[14,15] but it can be greatly facilitated if the protein shape is known because recent programs based on rigorous hydrodynamic theory can be used to calculate the global tumbling from the protein shape.[16]

Global shape optimization has not yet been introduced in the structure determination process due in part to the lack of fast computational methods for calculating the relevant observables from a given structure. In addition, the availability of an analytical function allowing the calculation of the overall orientation and the individual dipolar couplings from any given three-dimensional structure would greatly facilitate the pos-

* To whom correspondence should be addressed. E-mail: jgt@um.es; mpons@qo.ub.es.
† Universidad de Murcia.
‡ These authors contributed equally to this work.
§ Universitat de Barcelona.

(1) Tjandra, N.; Bax, A. *Science* **1997**, *278*, 1111−1114.
(2) Clore, G. M.; Gronenborn, A. M. *Proc. Natl. Acad. Sci. U.S.A.* **1998**, *95*, 5891−5898.
(3) Prestegard, J. H. *Nat. Struct. Biol*. **1998**, *5*, 517−522.
(4) Olejniczak, E. T.; Meadows, R. P.; Wang, H.; Cai, M.; Nettesheim, D. G.; Fesik, S. W. *J. Am. Chem. Soc.* **1999**, *121*, 9249−9250.
(5) Clore, G. M.; Starich, M. R.; Bewley, C. A.; Cai, M.; Kuszewski, J. *J. Am. Chem. Soc* **1999**, *121*, 6513−6514.
(6) Clore, M. G.; Garrett, D. S. *J. Am. Chem. Soc*. **1999**, *121*, 9008−9012.
(7) Delaglio, F.; Kontaxis, G.; Bax, A. *J. Am. Chem. Soc.* **2000**, *122*, 2142−2143.
(8) Hus, J.-C.; Marion, D.; Blackledge, M. *J. Am. Chem. Soc.* **2001**, *123*, 1541−1542.
(9) Hus, J.-C.; Marion, D.; Blackledge, M. *J. Mol. Biol*. **2000**, *298*, 927−936.
(10) Mueller, G. A.; Choy, W. Y.; Yang, D.; Forman-Kay, J.; Venters, R. A.; Kay, L. *J. Mol. Biol*. **2000**, *300*, 197−212.
(11) Andrec, M.; Du, P.; Levy, R. M. *J. Am. Chem. Soc.* **2001**, *123*, 1222−1229.
(12) Fischer, M. W. F.; Losonczi, J. A.; Weaver, J. L.; Prestegard, J. H. *Biochemistry* **1999**, *38*, 9013−9022.
(13) Bewley, C. A.; Clore, M. G. *J. Am. Chem. Soc.* **2000**, *122*, 6009−6016.
(14) Osborne, M. J.; Wright, P. E. *J. Biomol. NMR* **2001**, *19*, 209−230.
(15) Ghose, R.; Fushman, D.; Cowburn, D. *J. Magn. Reson*. **2001**, *149*, 204−217.
(16) García de la Torre, J.; Huertas, M. L.; Carrasco, B. *J. Magn. Reson*. **2000**, *147*, 138−146.

10.1021/ja011361x CCC: $20.00
Published on Web 11/02/2001

sibility of using dipolar couplings for ab initio protein structure determination.

Measurement of residual dipolar couplings requires a partial orientation of the protein. This is usually achieved by weak interaction with diluted oriented particles, such as bicelles,[17] purple membrane fragments,[18,19] filamentous phages,[20,21] or cellulose microcrystals.[22] The interaction with uncharged bicelles is mainly sterical and thus reflects the global shape of the protein. This is corroborated by the good agreement between the experimental values and the simulation results of the orientation of the protein that takes into account the volume excluded by obstacles.[23]

The global shape of most natural proteins can be described, to a good approximation, by an ellipsoid. Local deviations of the actual rigid three-dimensional structure from the regular geometrical object will often be averaged out by fast dynamics of the surface side chains and by weak interactions with the orienting obstacle.

Lipid bilayers act primarily as a cellular permeability barrier and as a matrix for several bilayer constituents. Membrane proteins are the protagonists of most of the active processes performed by biological membranes. Membrane functions are, to a large degree, mediated by orientational or conformational changes that result in the activation (or deactivation) of membrane proteins, as for example the opening of a membrane channel. These structural reorganizations are often associated with a change in the orientation of the protein, which will in part be determined by its interaction with the plane of the membrane. Therefore, information concerning the orientation of proteins in cellular membranes becomes critical in elucidating mechanisms by which these changes modify functional characteristics of membrane proteins.

In this paper, we show that the global orientation of an ellipsoid by a planar obstacle can be calculated analytically with a simple expression. Moreover, we show that the use of the gyration tensor, calculated from the three-dimensional atomic-level structure of the protein, provides analytical predictions of the individual dipolar couplings that are in very good agreement with experiment and with the results of numerical calculations.

The organization of this paper is as follows. Our starting point is a general theory for the restrictions in position and orientation of particles coexisting with large obstacles, which is subsequently particularized to planar obstacles. An analytical solution of this problem is feasible for ellipsoidal particles. The concepts involved are simple, but the description of the physical and geometrical details is mathematically complex and lengthy. Therefore, we have presented that part of the work separately from the main body of this paper in an Appendix (see Supporting Information). Thus, in the following section we present directly the fundamental results for the orientation of ellipsoidal particles by planar obstacles, and then we proceed with the first practical application, in the problem of the orientational distribution of particles confined in a planar membrane. The order parameter for ellipsoidal particles is evaluated as a function of some ratios of particle dimensions and membrane thickness. Finally, we describe the calculation of order parameter and alignment tensor for a system of ellipsoidal particles oriented by a liquid crystalline suspension of platelets. The results are employed to predict NMR dipolar couplings of globular proteins oriented by bicelles. A procedure to calculate analytically the order parameter and the dipolar couplings in real proteins is described in detail, and examples of this application are presented and discussed.

General Aspects

The orientation of rigid hard particles by liquid crystals has been calculated in the past using a variety of models. Although both long-range and short-range interactions have been considered, repulsive interactions have been recognized as an important ordering mechanism. The shape of solutes, needed to calculate the orientation restrictions imposed by the liquid crystalline phase, has been introduced using hard parallelepipeds,[24] shape functions based on linear dimensions,[25] or by a second-rank tensor defined by analogy to the inertia tensor with group dimensions instead of masses.[26] The short-range interactions have been modeled as an elastic force opposing the displacement of a continuum mesophase[27] or by an orienting potential based on the angle between the surface normal and the mesophase director, integrated over the molecular surface.[28] Zweckstetter and Bax used an explicit representation of components of diluted mesophases as hard obstacles and calculated the induced orientation from the excluded space, using an atomic representation of the protein solute.[23] In this work, we also represent the mesophase as a planar obstacle but we model the shape of the protein to be oriented as an ellipsoid. This allows the analytical computation of the distribution of particle orientations.

The possible orientations of a rigid, hard particle in the presence of an oriented hard obstacle will depend on the distance from the particle to the obstacle, and the size and shape of both bodies will determine the form of the dependence. If the separation distance is beyond a certain limit, the distribution of orientations will be that typical of a free particle. Below that limit only some orientations are possible; this is the origin of the induced orientational ordering of the particle. Finally, there will be another limit below which the particle cannot be positioned.

In this work, we intend to obtain the distribution of particle orientations with reference to the Z axis of a laboratory-fixed coordinate system that coincides with the z axis normal to the planar obstacles. If the particles are axisymmetric, the orientation is specified just by the angle subtended by the symmetry axis and the Z direction, θ, with a probability density $g(\theta)$. Alternatively, we may use $c \equiv \cos\theta$ as the angular variable, with a probability density $p(c) \equiv g(c)/\sin\theta$. The orientational preference caused by the obstacles is measured by experimental properties that depend directly on the second moment of $p(c)$; the quantity that usually determines those properties is

(17) Bax, A.; Tjandra, N. *J. Biomol. NMR* **1997**, *10*, 289−292.
(18) Koening, B. W.; Hu, J.-S.; Ottiger, M.; Bose, S.; Hendler, R. W.; Bax, A. *J. Am. Chem. Soc.* **1999**, *121*, 1385−1386.
(19) Sass, J.; Cordier, F.; Hoffmann, A.; Rogowski, M.; Cousin, A.; Omichinski, JJ. G.; Löwen, H.; Grzesiek, S. *J. Am. Chem. Soc.* **1999**, *121*, 2047−2055.
(20) Clore, G. M.; Starich, M. R.; Gronenborn, A. M. *J. Am. Chem. Soc.* **1998**, *120*, 10571−10572.
(21) Hansen, M. R.; Müller, L.; Pardi, A. *Nat. Struct. Biol.* **1999**, *5*, 1065−1074.
(22) Fleming, K.; Gray, D.; Prasannan, S.; Matthews, S. *J. Am. Chem. Soc.* **2000**, *122*, 5224−5225.
(23) Zweckstetter, M.; Bax, A. *J. Am. Chem. Soc.* **2000**, *122*, 3791−3792.
(24) Straley, J. P. *Phys. Rev. A.*, **1974**, *10*, 1881−1887.
(25) Yim, C. T.; Gilson, D. F. R. *Can. J. Chem.*, **1990**, *68*, 875−880.
(26) Catalano, D.; Forte, C.; Veracini, C. A.; Zannoni, C. *Isr. J. Chem.*, **1983**, *23*, 283−289.
(27) Van der Est, A. J.; Kok, M. Y.; Burnell, E. E. *Mol. Phys.* **1987**, *60*, 397−413.
(28) Ferrarini, A.; Moro, G. J.; Nordio, P. L.; Luckhurst, G. R. *Mol. Phys.* **1992**, *77*, 1−15.

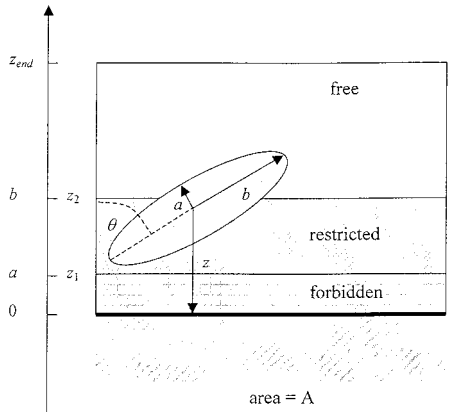

Figure 1. Side view of the system above one of the faces of a planar obstacle, showing the definition of the two main variables, z and θ, and the three possible regions.

the order parameter, S,

$$S \equiv \langle P_2(\cos\theta)\rangle = \frac{1}{2}(3\langle\cos^2\theta\rangle - 1) \tag{1}$$

where P_2 is the second Legendre polynomial, and

$$\langle c^2\rangle \equiv \langle\cos^2\theta\rangle = \int_0^{\pi} \mathrm{d}\theta g(\theta)\cos^2\theta = \int_{-1}^{+1} \mathrm{d}c c^2 p(c) \tag{2}$$

The derivation of the orientational distribution function begins with the formulation of a joint position−orientation distribution function that has to be integrated over the range of positional variables allowed within the system volume. For details, see section 1 in the Appendix.

Planar Obstacles and Ellipsoidal Particles

The systems considered in this work contain the following elements: (i) prolate ellipsoidal particles with semiaxes a, b, and $b > a$, with axial ratio $p = b/a > 1$, and (ii) planar obstacles, hereafter called planes or platelets. The dimensions of the plane are much larger than the largest particle dimension, so that end effects can be neglected. The reference frame system is obstacle-fixed, with its z axis perpendicular to the plane. The orientation of the ellipsoid is given by the angle θ subtended by its symmetry axis (that along b in the prolate ellipsoid) and z. Its position is defined by the distance along z from the center of the ellipsoid to the plane.

The system in which all our applications are based consists of a single plane of surface A and a system of volume, $V_t = Az_{end}$, where the particle's center may lie, above one of the faces of the plane limited by a height z_{end} over the plane (Figure 1). Up to three regions can be distinguished within this volume. From $z = 0$ to $z = a$, we have a forbidden region that is absolutely excluded for the particle's center, because within it the ellipsoid and the obstacle overlap necessarily; its volume is $V_b = Aa$. Between $z = a$ and $z = b$, we have a region where the orientation of the particle is restricted: a given value of θ is either possible or impossible depending on the value of z. Finally, beyond $z = b$ and up to z_{end}, there is a region where the orientation of the particle is not conditioned by the obstacle and adopts the distribution corresponding to free particles. We must consider two cases: (i) when $z_{end} > b$ as in Figure 1, with $V_r = A(b - a)$ and $V_f = A(z_{end} - b)$ and (ii) when $z_{end} < b$; in the latter case, the restricted region is not as large as it could be, $V_r = A(z_{end} - a)$ and there is no free region, i.e., $V_f = 0$.

For a system with distinct regions, $p(c)$, $\langle c^2\rangle$, and S can be evaluated as a sum of contributions from each region (see Appendix, section 1). In the unconstrained region (f), $p_f(c)$ is uniform and $\langle c^2\rangle_f = {}^1/_3$. Then, the problem reduces to the evaluation of, $p_r(c)$ and $\langle c^2\rangle_r$. This is described in the Appendix, with the results given by eqs A40 and A41. When the results for both regions are combined, we arrive at the final expressions. The normalized probability density for $c \equiv \cos\theta$ is

$$p(c) = 2\pi QA\{z_{end} - b[(1 - p^{-2})c^2 + p^{-2}]^{1/2}\} \tag{3}$$

and the second moment of the distribution is

$$\langle c^2\rangle = \frac{\frac{c_0^3}{3}z_{end} - bI_2(p,c_0)}{c_0 z_{end} - bI_0(p,c_0)} \tag{4}$$

Q is a numerical constant determined by the normalization of $p(c)$.

$$Q = \{4\pi A[c_0 z_{end} - bI_0(p,c_0)]^{-1}\} \tag{5}$$

The result of Q is only needed to evaluate $p(c)$. It does not enter in the calculation of $\langle c^2\rangle$ and S. Instead of z_{end}, region volumes can be used in eqs 3−5. Note that $z_{end} = V_t/A = (V_b + V_r + V_f)/A$, with $V_f = 0$ if $z_{end} < b$.

In eqs 3−5 we introduced the functions

$$I_n(p,x) = \int_0^x \mathrm{d}c c^n \sqrt{p^{-2} + (1 - p^{-2})c^2} \tag{6}$$

for which analytical results can be formulated (eqs 2.272.2 and 2.271.3 in Gradshteyn and Ryzhik.[29]):

$$I_0(p,x) = \frac{xu}{2} + \frac{p^{-2}}{2\sqrt{1 - p^{-2}}}\ln\frac{x\sqrt{1 - p^{-2}} + u}{p^{-1}} \tag{7a}$$

and

$$I_2(p,x) = \frac{xu^3}{4(1 - p^{-2})} - \frac{p^{-2}xu}{8(1 - p^{-2})} - \frac{p^{-4}}{8(1 - p^{-2})^{3/2}}\ln\frac{\sqrt{1 - p^{-2}} + u}{p^{-1}} \tag{7b}$$

with u being a shorthand notation for

$$u = \sqrt{p^{-2} + (1 - p^{-2})x^2} \tag{8}$$

V_f and V_r are the volumes of the free and restricted regions, respectively, and c_0 is a value that limits $\cos\theta$ within the interval $(-c_0, +c_0)$. The expressions for these quantities depend on which of the two following cases apply:

if $z_{end} > b$, $V_f = A(z_{end} - b)$, $V_r = A(b - a)$, and $c_0 = 1$

if $z_{end} < b$, $V_f = 0$, $V_r = A(z_{end} - a)$, and

$$c_0 = \left(\frac{z_{end}^2 - a^2}{b^2 - a^2}\right)^{1/2} \tag{9}$$

The above results provide a complete description of the orientation of the ellipsoidal particles referred to the local z axis

(29) Gradshteyn, I. S.; Ryzhik, I. M. *Table of Integrals, Series and Products*; Academic Press: New York, 1980.

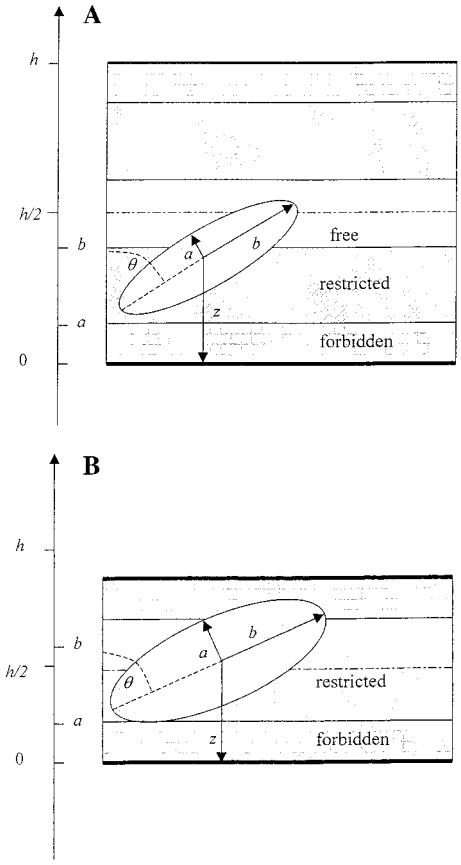

Figure 2. Ellipsoidal particle within a planar membrane of thickness $h = 2z_{end}$, in the two cases $z_{end} > b$ and $z_{end} <$ b, showing the different regions. (A) case with $h >$ 2b, showing a free region. (B) Case with $h < 2b$, without a free region.

normal to the plane. For more details, see sections 3 and 4 of the Appendix.

Particle Embedded in a Planar Membrane

A particular application of the results presented in the previous section concerns the orientation of an ellipsoidal particle embedded in the volume confined by the two parallel interfaces of a lipid bilayer. We suppose that the membrane is a planar layer of thickness h (Figure 2). The system volume, comprised between the two hard walls, can be divided into two equivalent subsystems of height $z_{end} = h/2$, each of which can be represented by the volume at one of the planar faces considered in the preceding section. Thus, eqs 3−5 apply to the present case. Again, we can distinguish two situations corresponding to (i) $h > 2b$, with the largest possible restricted region, and (ii) $h < 2b$, with a shorter restricted region and no free region (Figure 2A and B, respectively). The main results are

$$\text{if } h > 2b, \quad c_0 = 1, \quad \text{and} \quad S = \frac{I_0(p,1) - 3I_2(p,1)}{2[h/2b - I_0(p,1)]} \tag{10}$$

if $h < 2b$, c_0 is given by eq 9 and

$$S = \frac{(h/2b)(c_0^3 - c_0) + I_0(p,c_0) - 3I_2(p,c_0)}{2[(h/2b)c_0 - I_0(p,c_0)]} \tag{11}$$

Previously, the problem of orientation of elongated particles confined in a membrane was treated and analytically solved by

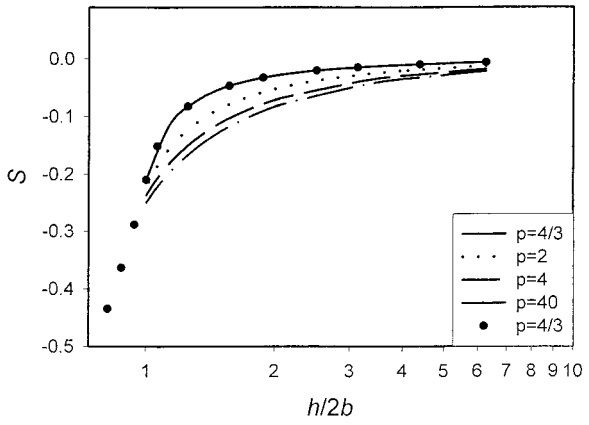

Figure 3. Order parameter, S, for a prolate ellipsoid ($p = b/a > 1$) embedded in a membrane of thickness h. The various curves, from top to bottom correspond to $p = {}^4/_3$, 2, 4, and 40. Note that the lowest possible value of h/b is $a/b = 1/p$. The data points are results of simulations for $p = {}^4/_3$ (the error bars are smaller than the size of the points).

Huertas et al.[30] for the special case of a very thin and long rod of length L, with the following results:

$$S = \frac{-1}{8(h/L) - 4} \qquad (h > L) \tag{12}$$

or

$$S = -\frac{1}{2}[1 - 1/2(h/L)^2] \qquad (h \le L) \tag{13}$$

These results are a particular case of our present more general treatment, making $L = 2b$ in the limit of $p \to \infty$. In this limit, we have $I_0(\infty, x) = x^2/2$ and $I_2(\infty, x) = x^4/4$. Placing these values into eqs 10 and 11, we reproduce the results of Huertas et al.[30]

The dependence of the order parameter, S, on the geometrical dimensions of the system can be illustrated by graphing numerical data from eqs 6−11. In Figure 3 we present the dependence of S on the ratio of the membrane thickness, h, to the longest particle dimension, $2b$, with different values of the axial ratio. The values of S go from 0, for very thick membranes, to −0.5, proper of a perpendicular orientation, when $h = 2a$, below which the particle just does not fit within the membrane.

The above-mentioned limiting value for the long rod is a good check of the correctness of our theoretical results, which were obtained after lengthy algebra (see Appendix). Anyhow, at this point we have conducted a numerical verification of our equations, comparing their numerical results with those of a simulation that is simple and fast for our problem. Simulation results, plotted along with the theoretical ones in Figure 3, confirm the validity of the latter.

Alignment by Liquid Crystalline Bicelles

Alignment of globular proteins, for the determination of NMR dipolar couplings, can be achieved in a dilute liquid crystalline suspension of bicelles, which play the role of the planar obstacles in our theory. Bicelles are phospholipid micelles of discoidal shape with a diameter that is large compared to their thickness.[31] The proteins are represented by ellipsoidal particles. As discussed below, this is an acceptable representation of the globular shape of many proteins.

(30) Huertas, M. L.; Cruz V.; López Cascales J. J.; Acuña A. U.; García de la Torre J. *Biophys. J.* **1996**, *71*, 1428−1439.

(31) Vold, R. R.; Prosser, R. S. *J. Magn. Reson. B* **1996**, *113*, 267−271.

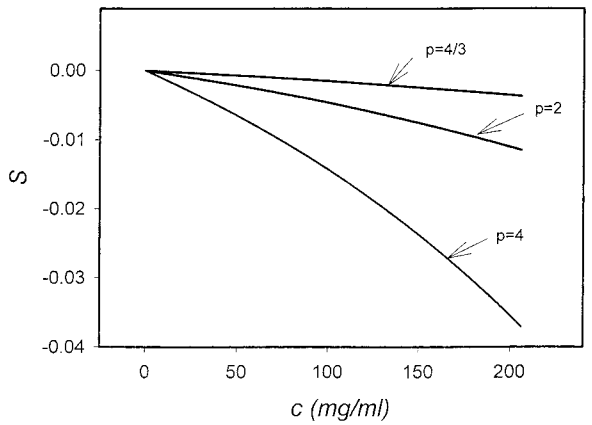

Figure 4. Order parameter, *S*, for prolate ellipsoids oriented by a dilute suspension of bicelles as a function of the lipid mass concentration *c* (the reference direction is the normal to the membrane plane).

Let us call *C* the known mass concentration of bicelles. Their volume fraction is $\upsilon = C/\rho$, where ρ is their density. If the total volume of the system is *V*, the volume occupied by the bicelles is $V_p = \upsilon V$ and the total planar area of the bicelles can be assumed to be $A = 2\upsilon V/\delta$, where δ is the thickness of the bicelle. This area defines a forbidden and a restricted region. The total volumes of the forbidden and restricted regions are $V_b = 2\upsilon Va/\delta$ and $V_r = 2\upsilon V(b - a)$.[32] The parameter z_{end} in eqs 3−5, which defines the maximum distance from the surface of the planar obstacle, can be calculated from the ratio between the volume not occupied by the bicelles ($V_t = V - V_p$) and the area *A*.

$$\frac{V_t}{A} = \delta\frac{\upsilon^{-1} - 1}{2} \tag{14}$$

Finally, $c_0 = 1$ since the restricted region has the largest possible thickness ($b - a$). Thus, for this problem, the orientational statistics is determined by a distribution function

$$p(c) = \frac{(\delta/2)(\upsilon^{-1} - 1) - b[(1 - p^{-2})c^2 - p^{-2}]^{1/2}}{2[\delta/2(\upsilon^{-1} - 1) - bI_0(p,1)]} \tag{15}$$

and an order parameter

$$S_{perp} = \frac{-[3I_2(p,1) - I_0(p,1)]}{2[(\delta/2b)(\upsilon^{-1} - 1) - I_0(p,1)]} \tag{16}$$

where the subscript perp indicates that the direction of reference is perpendicular to the planar obstacles, as we have been assuming so far. The calculated order parameters for ellipsoids with different axial ratios are plotted as a function of the lipid mass concentration in Figure 4.

Dipolar Couplings in NMR Spectroscopy

The dipolar coupling, D_{PQ}, between a pair of spin $^1/_2$ nuclei, P and Q, separated by a distance r_{PQ}, is related to the degree of orientation of the vector joining the two nuclei with respect to the direction of the magnetic field:

$$D_{PQ} = \left[\frac{\mu_0\gamma_P\gamma_Q h}{8\pi^3\langle r_{PQ}^{\ 3}\rangle}\right]d_{PQ} \tag{17}$$

where μ_0 is the vacuum magnetic permittivity, γ_P and γ_Q are the gyromagnetic ratios, *h* is Planck's constant, and d_{PQ} is a dimensionless quantity, with a maximum value of unity, that describes the degree of orientation of the **PQ** vector with respect to the magnetic field. The quantity d_{PQ} can expressed as the product $d_{PQ} = -S_{LS}S_{mol}$, where

$$S_{mol} = S_{corr}\sum_i\sum_j A_{ij}\cos\nu_i^{PQ}\cos\nu_j^{PQ} = S_{corr}\mathbf{v}_{PQ}^{\ T}\cdot\mathbf{A}\cdot\mathbf{v}_{PQ} \tag{18}$$

$$(i, j = 1, 2, 3 \text{ or } x, y, z)$$

and S_{LS} is the Lipari−Szabo generalized order parameter, usually not far from unity, which accounts for the effect of fast, low-amplitude motion of the internuclear vector. In eq 18, $\mathbf{v} = (\cos\nu_1^{PQ},\cos\nu_2^{PQ},\cos\nu_3^{PQ})$ is a unitary vector in the direction of vector **PQ**, which makes angles ν_1^{PQ}, ν_2^{PQ}, and ν_3^{PQ} with the particle fixed axes. A_{ij} are the components of the alignment tensor, **A**, given by

$$A_{ij} = \frac{1}{2}\langle 3\cos\theta_i\cos\theta_j - \delta_{ij}\rangle \tag{19}$$

$$(i, j = x, y, z \quad \text{and} \quad \delta_{ij} = 1 \quad \text{if} \quad i = j \quad \text{and} \quad \delta_{ij} = 0 \quad \text{if} \quad i \neq j)$$

where θ_i is the angle between the molecular axis *i* and the direction of the external magnetic field, which is taken as the laboratory *Z* axis. The brackets indicate an average obtained from the orientational statistics of the particle. The **A** tensor and hence S_{mol} are to be calculated according to the specific model for the particle alignment, in our case, the liquid crystalline array of bicelles. Following other authors,[23] small deviations of the real system from the orientational model are accounted for by the introduction of a correction factor, here denoted as S_{corr}, that will be close to unity (typically 0.8 [23]).

The alignment tensor, **A**, can also be characterized by its axial, A_a, and rhombic, A_r, components defined in terms of its eigenvalues as $A_a = {}^1/_3[A_z - (A_x + A_y)/2]$ and $A_r = {}^1/_3(A_x - A_y)$, where the order of the eigenvalues is $|A_z| > |A_y| > |A_x|$. The rhombicity, defined as $R = A_r/A_a$.

The generalized degree of order[33,34]

$$\Theta = \sqrt{\frac{2}{3}\sum_i\sum_j A_{ij}^{\ 2}} \tag{20}$$

is an invariant of the second-rank tensor **A** and, therefore, can be written in terms of the eigenvalues of **A** as $\Theta = [2(A_x^2 + A_y^2 + A_z^2)/3]^{1/2}$. The generalized degree of order characterizes the alignment of the molecules by a single quantity.

Bicelles are oriented in a magnetic field with their normal direction, i.e., the *z* direction of the frame of reference used so far, perpendicular to the field.[35] Therefore, the orientation angle whose cosine gives the order parameter is the complement of the angle that we had been considering so far. The new orientational average and order parameter, S_{para}, can be calcu-

(32) As the suspension of bicelles is dilute, we can assume that the separation between neighbor planes is appreciably greater than the longest particle dimension. This is quite reasonable, because the proteins studied by NMR are usually below 30 kDa, with a longest length of about 40 Å. As the separation between bicelles is large, the regions corresponding to neighbor platelets will not overlap, and the restricted region of a platelet of area A_1 will have the largest possible thickness ($b - a$), with $c_0 = 1$ and volume, $A_1(b - a)$. Additionally, in dilute suspensions, the relative orientation of different bicelles is irrelevant.

(33) Prestegard, J. H. *Biol. Magn. Reson.* **1999**, *17*, 311−355.
(34) Prestegard, J. H.; Al-Hashimi, H. M.; Tolman, J. R. *Q. Rev. Biophys.* **2000**, *33*, 371−424.

lated for this angle as described in section 5 of the Appendix, with the result expressed as

$$S_{\text{para}} = \frac{[3I_2(p,1) - I_0(p,1)]}{4[(\delta/2b)(\upsilon^{-1} - 1) - I_0(p,1)]} \tag{21}$$

This expression explicitly includes the averaging resulting from rotational disorder of the bicelle normal in the plane perpendicular to the magnetic field.

The alignment tensor of any axially symmetric particle is diagonal and determined by the order parameter of the symmetry axis of the particle with respect to the laboratory Z axis, S_{para} and given by

$$\mathbf{A} = \begin{pmatrix} -S_{\text{para}}/2 & 0 & 0 \\ 0 & -S_{\text{para}}/2 & 0 \\ 0 & 0 & S_{\text{para}} \end{pmatrix} \tag{22}$$

Therefore, we have $A_a = A_z/2 = S_{\text{para}}/2$ and the generalized degree of order is $\Theta = S_{\text{para}}$.

Individual dipolar couplings, from different internuclear vectors within the molecule, can be calculated by writing $\mathbf{v}^T \cdot \mathbf{A} \cdot \mathbf{v}$ in terms of the orientation of the vector with respect to the molecular axis. The details are described in section 6 of the Appendix. Here we just mention the main results. The main contribution to molecular order parameter for vector **PQ** takes the form $\mathbf{v}^T \cdot \mathbf{A} \cdot \mathbf{v} = S_{\text{para}} S_{\text{vec}}$, with

$$S_{\text{vec}} = \frac{3\cos^2\alpha_{\text{PQ}} - 1}{2} \tag{23}$$

where α_{PQ} is the angle subtended by vector **PQ** and the main axis of the axially symmetrical ellipsoid. Substituting this result in eq 18 leads us to $d_{\text{PQ}} = -S_{\text{LS}} S_{\text{corr}} S_{\text{para}} S_{\text{vec}}$. With the value for the order parameter given by eq 23, we obtain the explicit result for the expected attenuation from its maximum value of the dipolar coupling between two nuclei P and Q in an ellipsoidal particle

$$d_{\text{PQ}} = -S_{\text{LS}} S_{\text{corr}} \frac{(3\cos^2\alpha_{\text{PQ}} - 1)}{2} \frac{[3I_2(p,1) - I_0(p,1)]}{4[(\delta/2b)(\upsilon^{-1} - 1) - I_0(p,1)]} \tag{24}$$

Thus, the information needed for the calculation of D_{PQ}, apart from physical constants, is the following: the volume fraction and thickness of the bicelles, υ and δ ; the axial longest length and axial ratio of the particle, $2b$ and p; for each PQ vector, its angle α_{PQ} with the main particle axis; and finally, the generalized order parameter S_{LS} that is usually available from other NMR experiments. The functions $I_2(p,1)$ and $I_0(p,1)$ are given by eqs 6 and 7.

Our general result can be further simplified for some limiting cases that may be valid in practice. Thus, if the suspension of bicelles is very dilute, then the denominator of eq 16 reduces to $\delta/(b\upsilon)$. Another limit is when the overall shape of the particles is nearly spherical, represented by ellipsoid with p close to 1. A series expansion of $I_2(p,1)$ and $I_0(p,1)$ around $p = 1$ (see Appendix, section 4) leads to the result $3I_2(p,1) - I_0(p,1) = (^4/_{15})q$, with $q = p - 1$. If both limits (very dilute suspension of bicelles and nearly spherical particles) are applicable, we obtain an extremely compact and simple result:

$$d_{\text{PQ}} = -S_{\text{LS}} S_{\text{corr}} \frac{3\cos^2\alpha_{\text{PQ}} - 1}{2} \upsilon \frac{2b}{\delta} \frac{2}{15} q \tag{25}$$

In those conditions, the dipolar coupling is proportional to the volume fraction of the platelets, proportional to the ratio of the longest particle dimension to the bicelle thickness, proportional to the anisommetry measured by q, and the constant $^2/_{15}$, proper of the ellipsoidal geometry, will not be much different for nonellipsoidal geometry. Equation 25 predicts the order of magnitude of d_{PQ} for typical protein−bicelle systems: if $S_{\text{LS}} = 0.85$, $S_{\text{corr}} = 0.8$, $\cos\alpha_{\text{PQ}} = 1$ (maximum), $\upsilon = 0.05$, and $\delta = 40$ Å for the bicelles and $2b = 40$ Å with $p = 1.5$ for the protein, we find $d_{\text{PQ}} = -0.0023$, of the range of 10^{-3}−10^{-2}. Calculation of d_{PQ} using the complete eq 24 is very fast, since I_2 and I_0 are simple analytical expressions, and has been incorporated in the computer program that performs the whole calculation of d_{PQ} from the three-dimensional structure of a protein, as described below.

Ellipsoidal Representation of a Rigid Particle

The application of our analytical procedure to real proteins requires a representation of the particle by a prolate, revolution ellipsoid. For globular proteins, such a representation is acceptable since their shape is compact, not far from spherical, and it is well known that they are mostly prolate.[36−38] Various physical criteria could be used for the equivalence; we adopt a simple and reasonable choice based on the equivalence of the moments of inertia. Specifically, we consider the gyration tensor defined, for a system of N discrete, identical pointlike elements, as

$$\mathbf{G}_{\alpha\beta} = \frac{1}{N} \sum_{i=1}^{N} s_i^{(\alpha)} s_j^{(\beta)} \qquad (\alpha, \beta = x, y, z) \tag{26}$$

where $\mathbf{s}_i$ is the vector going from the particle's center of mass to the position of the ith element. The particle is discretized by three-dimensionally superimposing it to a hexagonal, closest packed lattice; the lattice nodes that fall within the particle are the elements to be used in eq 26. The rigid particle is initially represented by a set of overlapping spheres, representing individual extended (non-hydrogen) atoms, whose radii are taken identical for simplicity, with a value of about 2 Å, close to typical van der Waals radii of extended atoms. The spacing of the lattice is about 0.5 Å. This modeling procedure follows closely that employed to build the so-called filling model in hydrodynamic calculations.[39,40]

The gyration tensor calculated for all the nodes belonging to the particle is diagonalized to obtain its three eigenvalues, which for the reasons described below are denoted in the order $G_z > G_x > G_y$, and we obtain also the corresponding eigenvectors.

(35) Modified bicelles that are oriented with their normal in the direction of the field can also be produced by the addition of lanthanides or lipids modified with aromatic groups. In this case, the order parameter would be S_{perp}, given by eq 16. However, the application reported here is for the more frequent case, governed by eq 21. Other orienting systems, such as rodlike phages, form liquid crystalline phases and the present equations would not apply. In addition, typical phage systems are charged and induce orientation mainly by electrostatic effects. Modifications to include electrostatic effects are presently being developed.

(36) Tanford, C. *Physical Chemistry of Macromolecules*; Wiley: New York, 1961; Chapter 6.
(37) Harding, S. E.; Rowe, A. J. *Int. J. Biol. Macromol.* **1982**, *4*, 160.
(38) Harding, S. E.; Cölfen, H. *Anal. Biochem.* **1995**, *228*, 131.
(39) García de la Torre, J.; Huertas, M. L.; Carrasco, B. *Biophys. J.* **2000**, *78*, 719−730.
(40) Carrasco, B.; Garcia de la Torre, J. *Biophys. J.* **1999**, *76*, 3044−3057.

The molecule will be adequately represented by a revolution ellipsoid when two of the eigenvalues are quite similar, while the other is appreciably distinct. The shape is prolate when the unique eigenvalue is the largest one, G_z, and $G_x \approx G_y$. The eigenvalues of the gyration tensor of a prolate ellipsoid with semiaxes $b > a = a$ are $G_z = b^2/5$ and $G_y = G_x = a^2/5$. Thus, our choice for the equivalent ellipsoid is that with $b = (5G_z)^{1/2}$ and $a = [5(G_x + G_y)/2]^{1/2}$. Furthermore, the eigenvalue corresponding to G_z gives the orientation of the symmetry (long) axis of the ellipsoid (needed to calculate α_{PQ} for eq 23).[41] R_g has been proposed as a useful constrain in structural refinements.[42]

Rhombicity Correction

As revealed by the analysis of experimental data (vide infra), the revolution ellipsoid provides an acceptable prediction of the dipolar couplings for proteins that conform approximately to this axially symmetrical model. Geometrically this happens when the minor eigenvalues of the gyration tensor are similar, $G_x \approx G_y$, and results in an alignment tensor are $A_x \approx A_y$. To account adequately for cases in which this situation does not hold, we have devised a correction with a perturbative point of view. The generalized degree of order for a rhombic structure can be written as

$$\Theta = 2A_a\sqrt{1 + \frac{4}{27}R^2} \tag{27}$$

For typical values of R, the departure of Θ from its value in an axially symmetrical system ($2A_a$) is solely in the order of a few percent. It is therefore justified to take the values obtained for the axially symmetrical model as a first-order approach and to introduce the rhombicity correction a posteriori in a perturbative fashion.

The procedure, which is based on the rhombicity treatment of the dipolar coupling and alignment tensors by Clore et al.,[43,44] is described in detail in the Appendix (see Supporting Information). Here we just describe the main aspects. From eq 1 of Clore et al.,[44] the dipolar couplings for a case of nonvanishing rhombicity can be written as

$$D^{PQ}(R) = \rho D^{PQ}(0) \tag{28}$$

where

$$\rho = 1 + \frac{3}{2}R\frac{\sin^2\alpha\cos^2 2\beta}{3\cos^2\beta - 1} \tag{29}$$

and

$$R = \frac{A_x - A_y}{A_z - (A_x + A_y)/2} \tag{30}$$

In eq 28, $D^{PQ}(R)$ is the dipolar coupling associated with an internuclear vector PQ in the general case and $D^{PQ}(0)$ is the value that would correspond to a particle with the same axial (z) eigenvalue and eigenvector, but with degenerated eigenvalues in the other two directions. R is the rhombicity, and α and β in eq 29 are the polar angles of the PQ vector.[45]

Considering that the shape of the particle is similarly reflected in the alignment, **A**, and gyration, **G**, tensors, we assume that the rhombicity of the eigenvectors of both tensors should be similar. Therefore, we formulate the hypothesis that the rhombicity R to be used in eq 29 can be calculated as

$$R = \frac{G_x - G_y}{G_z - (G_x + G_y)/2} \tag{31}$$

using, as above, the criterion $G_z > G_x > G_y$, to ensure that R is positive.

In summary, the perturbative rhombicity correction consists of multiplying the dipolar coupling calculated with the axially symmetrical ellipsoid by the factor ρ of eq 29, using the rhombicity of the gyration tensor **G** and the polar angle β for each vector, measured from the eigenaxis corresponding to the intermediate eigenvalue of **G**.

Application to Experimental Systems

We have applied the analytical procedure for calculating dipolar couplings from three-dimensional structures to a number of unrelated proteins for which dipolar couplings have been measured in the presence of bicelles.[46−53] The results are summarized in Table 1. In all cases, there is a good to excellent agreement between theory and experiment and an excellent agreement between the dipolar couplings calculated using the analytical method and the exhaustive enumeration of conformations method of Zweckstetter and Bax.[23] For each protein, the principal values of the gyration tensor and the dimensions of the equivalent ellipsoid are reported.

To illustrate the application of our procedure for the calculation of dipolar couplings, we describe the case of the cellular factor BAF (barrier-to-autointegration), a 21 000 M_w dimer whose three-dimensional structure has been solved including an extensive use of dipolar couplings.[46] The three-dimensional mean regularized structure and the experimental restraints are available in PDB file 2ezx. Diagonalization of the gyration tensor yields eigenvalues $G_y = 49.6$, $G_x = 63.6$, and $G_z = 187.9$ and a radius of gyration of 17.35. From these, the dimensions of the semiaxes of the ellipsoid are $b = 30.7$ Å and $a = 16.8$ Å, with an axial ratio $p = 1.82$. The eigenvector associated with G_z provides the orientation of the ellipsoid in the coordinate axes of the PDB structure. The cos α_{PQ} values are obtained from the projection of the normalized internuclear NH vectors onto the z principal axis. The Lipari−Szabo order parameter was set to a typical value, $S_{LS} = 0.85$, for all NH bonds. The empirical constant S_{corr} that accounts for imperfect alignment of the bicelles was set to 0.8 following Zweckstetter−Bax.[23] The averaged mean NH distance was set to 1.04 Å. The volume fraction of bicelles was set to $\upsilon = 0.058$, assuming a density of 1.03 g/cm^3. The thickness of the bicelles was set to $\delta = 40$ Å.

Figure 5 shows a comparison of the experimental NH dipolar couplings with the results of the calculations using the analytical expression or the SSIA method.[23] Despite the drastic simplifica-

(41) The gyration tensor is closely related to the tensor of inertia; the eigenvectors of the inertial and gyration tensor are the same, and the principal moments of inertia are combinations of the eigenvalues of the gyration tensor: $I_x = G_y + G_z$, and so on. The trace of the inertia tensor is the squared radius of gyration, R_g. However, the gyration tensor gives a more faithful representation of the molecule shape, which is the factor that determines the orientation of proteins by bicelles.

(42) Kuszewski, J.; Gronenborn, A. M.; Clore, M. G. *J. Am. Chem. Soc.* **1999**, *121*, 2337−2338.

(43) Clore, G. M.; Gronenborn, A. M.; Tjandra, N. *J. Magn. Reson.* **1998**, *131*, 159−162.

(44) Clore, G. M.; Gronenborn, A. M.; Bax, A. *J. Magn. Reson.* **1998**, *133*, 216−221.

(45) As R and the axial eigenvalue A_z are defined as positive, the ordering of the other eigenvalues has to be $A_x > A_y$.

(46) Cai, M.; Huang, Y.; Zheng, R.; Wei, S.-Q.; Ghirlando, R.; Lee, M. S.; Craigie, R.; Groneneborn, A. M.; Clore, G. M. *Nat. Struct. Biol.* **1998**, *5*, 903−909.

Table 1. Calculation of NH Dipolar Couplings of Proteins in the Presence of Bicelles by an Analytical Procedure Using an Ellipsoidal Representation of Proteins. Correlation with Experimental and Simulation (SSIA) Results

		gyration tensor[a]			ellip model[b]		correlation	
protein	PDB code	G_z	G_x	G_y	*a*	*b*	$\mathbf{r}^2_{\text{anal vs exp}}$[c]	$\mathbf{r}^2_{\text{anal vs SSIA}}$[d]
BAF[46]	2ezx	187.9	63.62	49.65	16.8	30.7	0.97 (0.98)	0.97 (0.98)
cyanovirin-N[47]	2ezm	149.9	34.54	26.08	12.3	27.4	0.71 (0.68)	0.96 (0.97)
KH3[48]	1khm	151.9	56.59	27.62	14.5	27.6	0.81 (0.83)	0.95 (0.99)
GAIP[49]	1 cmz	177.1	35.76	17.71	15.1	29.8	0.91 (0.92)	0.92 (0.97)
ubiquitin[50]	1d3z	74.33	42.00	31.31	13.5	19.3	0.74 (0.72)	0.89 (0.93)
protein G domain[e 51]	1igd	64.39	29.10	20.90	11.2	17.9	0.97 (0.98)	0.97 (0.98)
protein G domain[52]	3gb1	67.03	30.15	22.06	11.4	18.3	0.94 (0.96)	0.97 (0.98)
lysozyme[53]	1e8l	108.8	48.42	43.64	15.2	23.3	[f]0.87 (0.90)	0.93 (0.93)

[a] The gyration tensor was calculated as explained in text. The eigenvalues are $G_z > G_x > G_y$. [b] Semiaxis of the ellipsoid model. $b > a$. *a* and *b* were calculated through the formulas specified in the text. [c] Experimental values obtained as a restrain file in the PDB. Values in parentheses correspond to correlation coefficients when rhombicity correction is used. [d] SSIA calculation data in bicelles: grid spacing 0.5 Å, ionic radii 3.1. Å, only heavy atoms used. Lipid concentration was the specified in the reference. Coordinates are from NMR structures unless stated otherwise. Values in parentheses correspond to correlation coefficients when rhombicity correction is used. [e] X-ray structure. [f] Experimental residual dipolar couplings corresponding to thr 7.5% w/v sample DMPC−DHPC−CTAB 2.9:1:0.1.

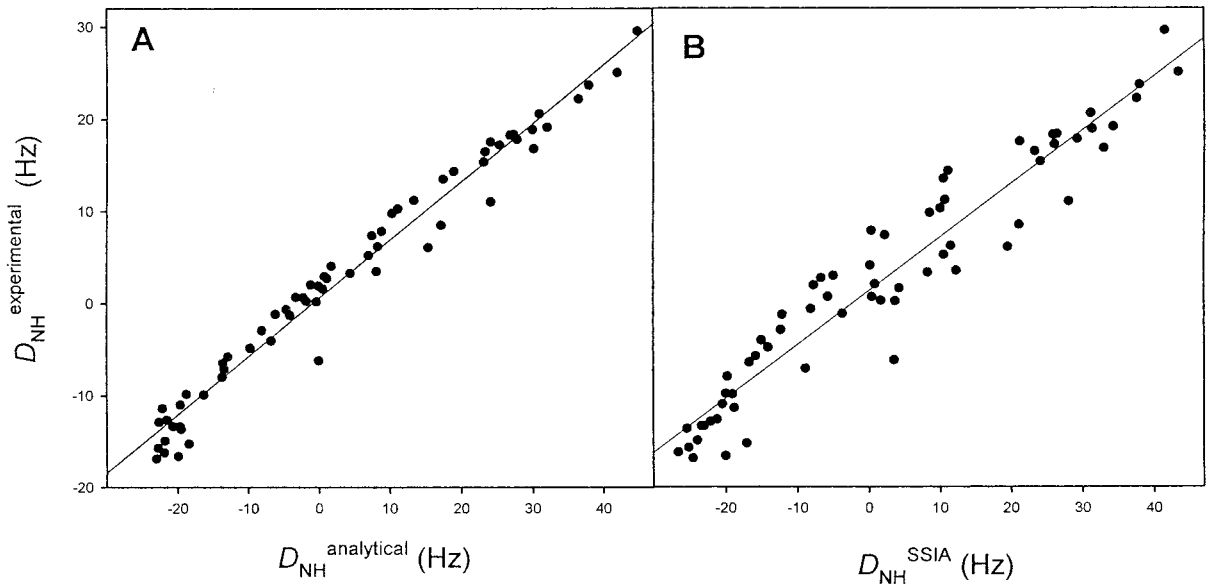

Figure 5. Residual dipolar couplings for factor BAF (barrier-to-autointegration) oriented using a 6% w/v suspension of DMPC−DHPC bicelles. Correlation between experimental and calculated D_{NH} using (A) the analytical expressions given in this work and (B) the SSIA program.[23]

tion implied in the assumption of an ellipsoidal shape, the analytical results are in very good agreement with the experimental results and give results comparable to those obtained with the program SSIA although at a computational cost 10.000 times smaller.

A comparison of the calculated values using our approximate analytical function and the exhaustive exploration of orientations of the SSIA program provide some insight on the applicability and limitations of our method. Figure 6 shows plots of dipolar couplings calculated by the two methods for four different proteins. In all cases, the regression lines have slopes close to 1 that pass through the origin and the regression coefficients are higher than 0.92. For proteins that have an appreciable rhombic component, the assumption of axial symmetry in the analytical calculation causes a triangular shape for the distribution of points in the plots for some of the proteins, such as cyanovirin-N.[47] The rhombic component introduces a higher dispersion in the dipolar couplings of NH vectors oriented perpendicular to the principal axis of the ellipsoid. The introduction of the correction the factor ρ defined by eq 29, improves dramatically the agreement between the calculated and predicted residual dipolar couplings. This improvement is shown in Figure 7 for the proteins KH3 and GAIP. The rhombicity correction also introduces a significant improvement in the correlation coefficients between the analytically calculated dipolar couplings and both the experimental values and the results from the SSIA program. This confirms the above interpretation and proves that the rhombicity effects can be effectively introduced in the analytical calculation of residual dipolar couplings.

For the smaller proteins, such as ubiquitin,[50] (not included in the figure) and protein G,[51,52] the agreement between the two methods tends to be poorer. This probably reflects the fact that local deviations from the regular geometrical shape have a stronger effect. In the case of protein G,[51,52] composed of a single β-sheet and a single α-helix, dipolar couplings calculated by the two methods give slightly different correlation lines for the NH groups located in the α-helix and in the β-sheet structural

(47) Bewley, C. A.; Gustafson, K. R.; Boyd, M. R.; Covell, D. G.; Bax, A.; Clore, G. M.; Gronenborn, A. M. *Nat. Struct. Biol.* **1998**, *5*, 571−578.

(48) Baber, J. L.; Libutti, D.; Levens, D.; Tjandra, N. *J. Mol. Biol.* **1999**, *289*, 949−962.

(49) de Alba, E.; De Vries, L.; Farquhar, M. G.; Tjandra, N. *J. Mol. Biol.* **1999**, *291*, 927−939.

(50) Ottiger, M.; Bax, A. *J. Am. Chem. Soc.* **1998**, *120*, 12334−12341.

(51) Derrick, J. P.; Wigley, D. B. *J. Mol. Biol.* **1994**, *243*, 906−918.

(52) Gronenborn, A. M.; Filpula, D. R.; Essig, N. Z.; Achari, A.; Whitlow, M.; Wingfield, P. T.; Clore, G. M. *Science* **1991**, *253*, 657−661.

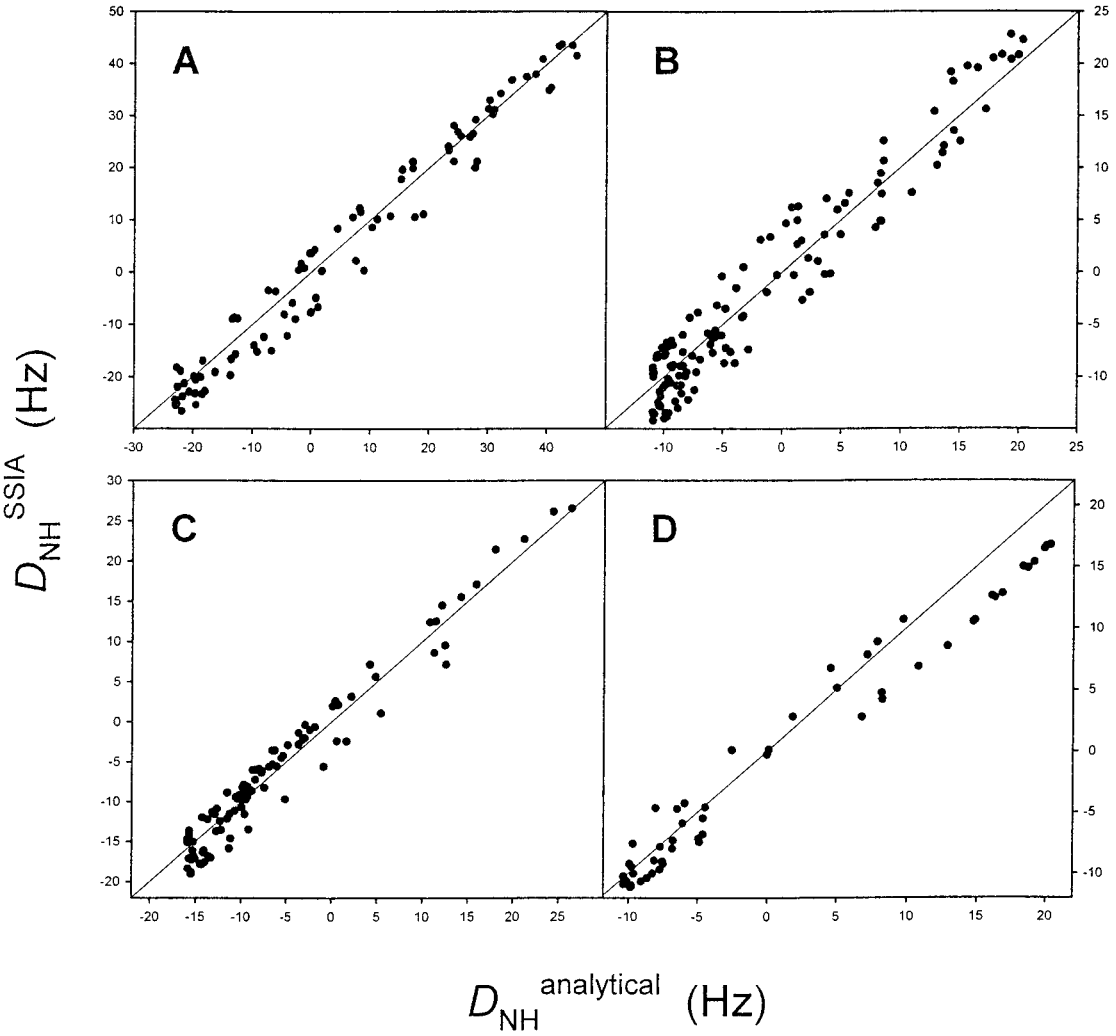

Figure 6. Comparison of residual dipolar couplings calculated using the analytical procedure described in this work and the SSIA program for the proteins: (A) BAF, (B) lysozyme, (C) cyanovirin-N, and (D) protein G domain X-ray structure. The coordinates were obtained from the PDB files indicated in Table 1.

elements. This can be explained by the strong correlation of the orientations of individual NH bonds within a secondary structure element and the fact that the subset of orientations that may be allowed in one of the models and not in the other contribute differently to the dipolar couplings of NH groups in different parts of the molecule.

The calculation assumes that the orientation has steric origin and that the distribution of protein molecules along the normal of the bicelle is uniform. Electrostatic effects can have an effect on both assumptions. Schwalbe et al.[53] studied the orientation of lysozyme by bicelles formed by 5% DMPC−DHPC (2.9:1) and DMPC−DHPC−CTAB (2.9:1:0.1). DMPC−DHPC bicelles, although formally neutral, are reported to have a slight negative charge as a result of partial hydrolysis of the phospholipid headgroups.[54] Addition of cetyltrimethylammonium bromide (CTAB) results in positively charged bicelles. Lysozyme has positive charge at pH 6.5. Figure 8 shows plots of the experimental versus calculated dipolar couplings for lysozyme oriented using 5% DMPC−DHPC (2.9:1) bicelles and 7.5% DMPC−DHPC−CTAB (2.9:1:0.1) bicelles. The slope of the regression line is 1.5 for the DMPC−DHPC and 0.7 for the positively charged bicelles. Deviations from the unit slope, beyond the experimental uncertainty in the amount of lipid added, can be explained by the electrostatic attraction/repulsion between the positively charged protein and the negatively/positively charged bicelles that increases/decreases the concentration of protein in the proximity of the bicelle where orientation is restricted. In addition, electrostatic interactions cause changes in the orientation of the steric alignment tensor. By comparing experimental and predicted dipolar couplings, a change in orientation of the alignment tensor with respect to the calculated one causes a poorer fit and a roughly ellipsoidal shape in the distribution of points. Triangular point distributions suggest that nonsteric effects are introducing an additional rhombic component.

Concluding Remarks

In this paper, we have derived expressions to calculate analytically the orientation acquired by a particle with the shape of a prolate ellipsoid interacting with a planar surface. The resulting expressions allow the calculation of the orientation of a particle embedded in a lipid bilayer or the calculation of the residual dipolar couplings expected from partially oriented globular proteins in the presence of bicelles.

The key assumption that the shape of a globular protein can be represented by an axially symmetrical ellipsoid is validated by the good agreement observed between residual dipolar

(53) Schwalbe, H.; Grimshaw, S. B.; Spencer, A.; Buck, M.; Boyd, J.; Dobson, C. M.; Redfield, C.; Smith, L. *Protein Sci.* **2001**, *10*, 677−688.

(54) Losonczi, J. A.; Prestegard, J. H. *J. Biomol. NMR* **1998**, *12*, 447−451.

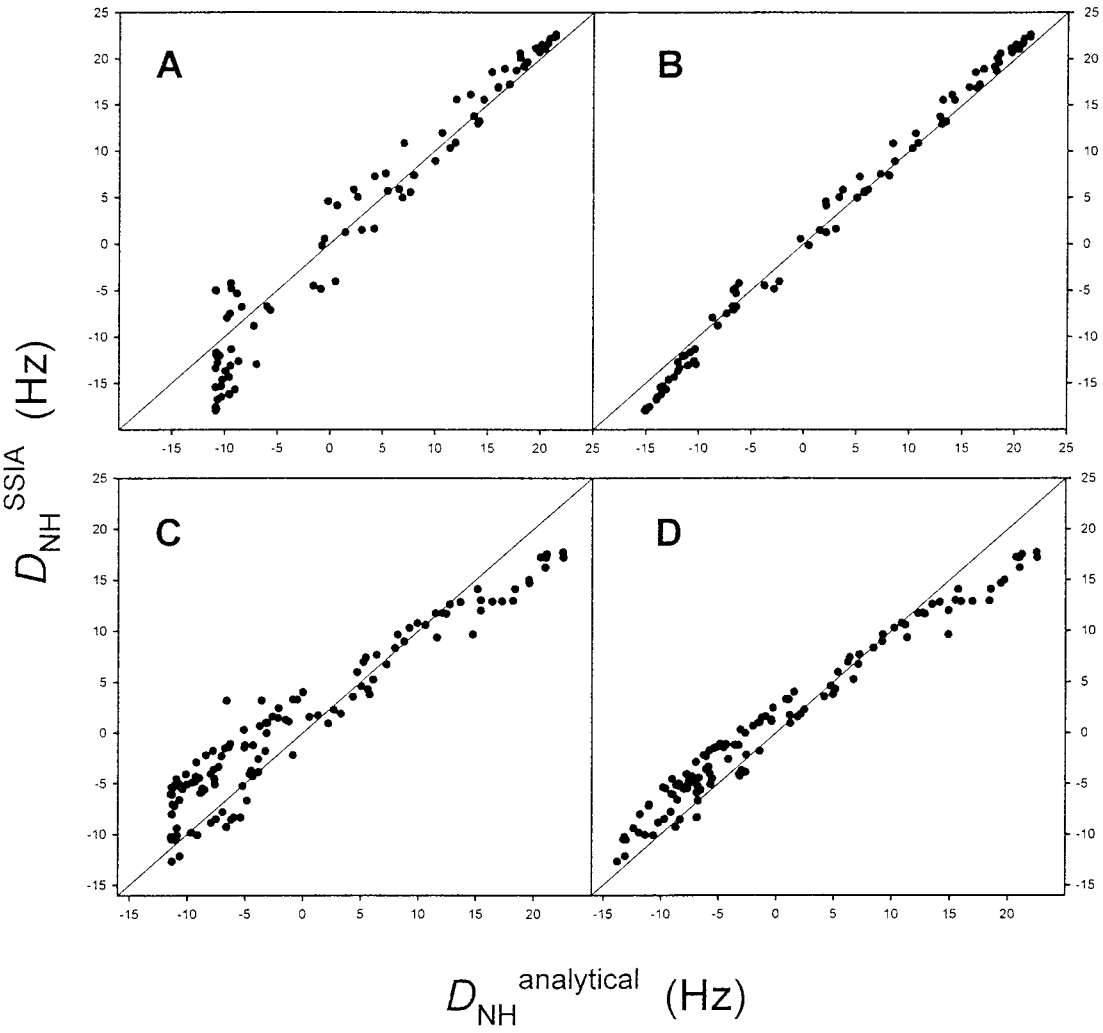

Figure 7. Comparison of residual dipolar couplings calculated using the analytical procedure described in this work (with and without rhombicity correction) and the SSIA program: (A) KH3 without rhombicity correction, (B) KH3 with rhombicity correction, (C) GAIP without rhombicity correction, and (D) GAIP with rhombicity correction.

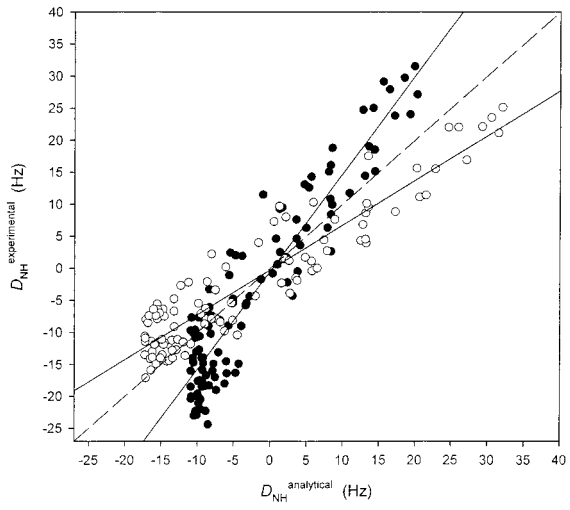

Figure 8. Comparison of experimental and analytically calculated residual dipolar couplings for lysozyme oriented in 5% DMPC−DHPC bicelles (full symbols) and 7.5% DMPC−DHPC−CTAB (2.9:1:0.1) bicelles (open symbols). The corresponding regression lines and a straight line with unitary slope are included.

couplings calculated analytically and those measured experimentally or calculated using a simulation that systematically explores all the allowed orientations of the protein.

The study of a number of proteins confirms the wide applicability of the analytical formulas. Known limitations include the assumption that the protein is prolate. The major limitation is the breakdown of the assumption that steric effects dominate the orientation. The simple expressions for the steric component should facilitate the introduction of additional orientation effects. Electrostatic interaction between charged proteins and charged obstacles is probably the most important of them, and we are presently working on analogous expressions to include electrostatic effects, as well as to calculate the effects of obstacles of different shapes, such as cylinders.

The decrease in computational cost of the analytical formulas opens the possibility of using global shape constraints derived from dipolar couplings in the initial stages of the structural determination procedure.

Acknowledgment. This work was partially supported by funds from the Spanish Ministerio de Ciencia y Tecnologia (Grant BQU2000-0229 to J.G.T. and Grant PB97-0933 to M.P.). M.P. acknowledges financial support from the Generalitat de Catalunya (Centre de Referencia de Biotecnologia i Grup Consolidat). P.B. is supported by a predoctoral grant of Ministerio de Educación, Cultura y Deportes. M.X.F. thanks Fundação para a Ciência e Tecnologia (Portugal) for Grant SFRH/BPD/3594/2000.

Supporting Information Available: A Microsoft Word document containing an appendix to this article describes a general theory of the orientation of rigid particles by planar obstacles, with a step-by-step deduction of the results reported in this work. This material is available at the author's Web site http://leonardo.fcu.um.es/macromol. A computer program that implements our procedure will be available from this address. This material is available free of charge via the Internet at http://pubs.acs.org. See any current masthead page for ordering information and Web access instructions.

JA011361X